Brief Description of DW Dynamic and assumptions about Bloch DW Dynamics

Kaijing Yin
Tutor: X. R. Wang
School of Physics & Electronics, Hunan University, Changsha, Hunan Province, 410006, China
Nitrogennn@hnu.edu.cn

Abstract

This article not only described the research process in DW Dynamics during the latest 15 years based on six works which have representativeness, but also expressed author' s assumption around the dynamics of Bloch DW in SOT at the condition without influences of DMI and external magnetic field and corrected some mistakes made by former researchers by using statistical physics. Specifically, statistical physics contributed to the correction by introducing probability density functions through the Fokker-Planck equation, thereby improving the description of Bloch DW stochastic dynamics. It also described what lacks in research of DW Dynamics nowadays and how to improve it.

Keywords: DW Dynamics; LLG Equation; Collective Coordinates; Statistical Physics; Fokker-Planck Equation

1. Introduction

The Magnetic Domain is a region within a magnetic material in which the magnetization is in a uniform direction, among it the parts which separate different magnetic domains are Domain Walls (Also called as DW as the title does). Among its sub-type the Bloch DW, as the DW I would like to study its dynamic characteristic carefully in the future, is a kind of DW which magnetic moment rotates within the wall surface, and the direction of magnetization changes along the normal of the wall surface, without free magnetic poles, while the N'eel DW has its magnetic moment rotates in the direction of the normal to the wall surface, its magnetization direction changes parallel to the wall surface, with surface free magnetic poles.

2. Description

In this part six important DW Dynamics researches along with figures which related to the results of study would be cited and introduced.

2.1 All-Magnonic Spin-Transfer Torque and DW Propagation (2010) [1]

This research is divided into theorical part and experimental part.

Firstly, in the theoretical derivation by using the method of LLG equation with unit vector of magnetization m stands for the unit direction which fits the relationship M=mMS with a saturation magnetization MS, with an magnon which angular momentum is h this research derivated that m only changes its direction, its value remained unchanged instead. Besides it also showed the width $\triangle = \sqrt{\frac{A}{K}}$(A: exchange coefficient, K: anisotropy coefficient), as illustrated in FIG. A.1:

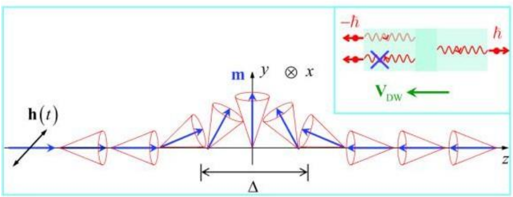

FIG. A. 1. Schematic representation of a domain wall profile and its width Δ.

Then by using another method as spherical coordinates to express m as mθ and mφ, along with using current density $J = \alpha m \times \frac{\partial}{\partial z} m$ to express LLG equation.Finally by using it and relationships such as $|Jz|=A\rho^2 k$ and $Jz = \frac{A}{2i\triangle}[\varphi \, \partial (\frac{z}{\triangle}) \, \varphi^* - \varphi^* \, \partial (\frac{z}{\triangle}) \, \varphi]$, the value of DW velocity can be calculated as $VDW = -\frac{\rho^2}{2} V_g \hat{z}$ which group velocity is $V_g = \frac{\partial \omega}{\partial k} = 2AK$.

The experimental part, conducted in a YIG magnet environment with parameters such as α and K⊥, examined the theory under conditions where damping and transverse magnetic anisotropy were absent. The results are shown in FIG. A. 2., FIG. A. 3. and FIG. A. 4.

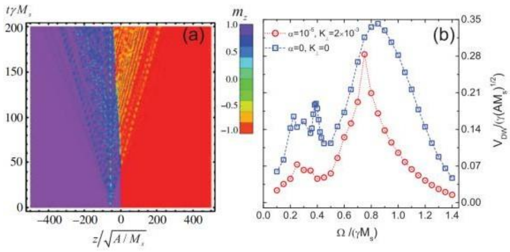

FIG. A. 2. (a)Density plot in the z-t plane at a frequency of Ω=0.75 for $K_\perp=2\times10^{-3}$ and α= 10^{-5}(YIG parameters). (b)The reliance of DW velocity on frequency. (Red circles: YIG parameters, blue squares: lacking damping and transverse magnetic anisotropy.

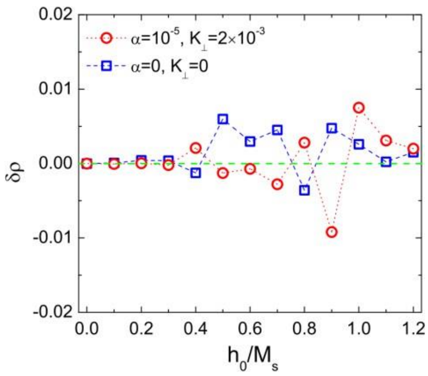

FIG. A. 3. Variations in spin-wave amplitude at two locations on the DW's opposite sides, influenced by the field. Red circles and blue squares stand for the same parameter as FIG. A. 2. Among these the red is at the optimal frequency(Ω=0.75), and the blue is also at its optimal frequency(Ω=0.85).

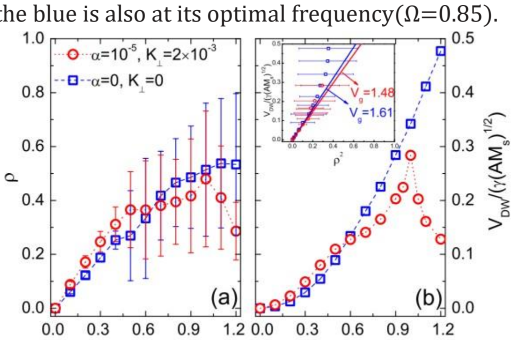

FIG. A. 4. (a) The reliance of spin-wave amplitude on the field for YIG parameters (indicated by red circles) at frequency Ω=0.75, compared to scenarios without damping and transverse magnetic anisotropy (shown as blue squares) at frequency Ω=0.85. (b) The reliance of the DW velocity on field under the same scenarios.

In conclusion, this research has a strong characteristic of processing from derivation to experiment, it also contains the advantage of having intuitive experimental verification and rigorous theoretical derivation logic, but it still involves quantum theory to a lesser extent.

2.2 Universal magnetic DW dynamics in the presence of weak disorder (2013) [2]

This research studied its theme such as to study the key physical quantities as DW velocity v, magnetic field intensity H, driving force f, where H involves discussions on the depinning field Hdep and f involves discussions on the depinning force fc by focusing on its important control variables as temperature T, thickness of the experimental carrier, where T covers discussions on T_{dep}.

This experiment mainly took place in the environment of thick Pt/Co film, used the model of 1D Model of DW Motion in a Defect-Free Ferromagnetic Layer which expression of mobility m in terms of DW velocity v and magnetic field intensity H is given under the condition of ignoring defects and referred the basic theory of research: Disorder Consequences on the Dynamics of a Single Ultrathin Ferromagnetic Layer and Mechanism of Field-Driven DW Motion.

As the result of studying field-driven DW dynamics and creep, Field-Driven Creep shown adjustable parameters in a single magnetic layer, Field-driven domain wall motion stood out for intra-layer interaction, Field-driven domain wall motion in magnetic coupling layers compared and summarized DW dynamics and Field-driven motion in confined geometries was also given a brief introduction.

When giving a summary about the influence of electric fields on DW motion, the expression in Electrically-driven wall motion for DW creep velocity under electric field-driven conditions is given based on the DW creep velocity formula as $\mathbf{v} = \mathbf{v}_0\exp[-(T/T_{dep})(\mathbf{H}/\mathbf{H}_{dep})^{\mu}]$, Electric field-assisted wall motion was also mentioned briefly.

This passage showed its advantages such as using relatively definite expressions to characterize DW velocity v with H and utilizing a large number of visual images to clearly and intuitively represent the relationship of physical quantities such as v-H, but its drawbacks such as not fully considering the possible influence of dielectric when in the electric field-driven environment and not taking the impact of the electromagnetic induction effect on the DW movement speed into account.

2.3 Thermal gradient driven DW dynamics (2018)[3]

This is a research which researched the value of m and current by focusing on thermal field (Easy-Axis Anisotropy K||).Among this experiment there came out the method of using LLG equation which contains $m=M/M_S$ to characterize the effective field H_{eff} and the thermal gradient ∇xT in the x-direction, as well as the spin current intensity J(x) in the environment of a uniaxial nanowire with a length of Lx, a cross-section of Ly along the x-axis (easy axis) × Lz, and a head-to-head double wall structure at the center. Among this The expression of H includes the dipole thermal field dipole (connecting magnetism and thermodynamics, corresponding to the research conditions of this paper), and the random thermal field hth follows a Gaussian process statistical distribution. Finally, the domain wall motion is characterized by vcurrent.

It carried out results below:

(a) Average spin current and DW velocity: FIG. C. 1. gave the variation law of the current density of the domain wall under different thermal gradients and different positions, vsimu and vcurrent and their relationship with the thermal gradient are obtained.

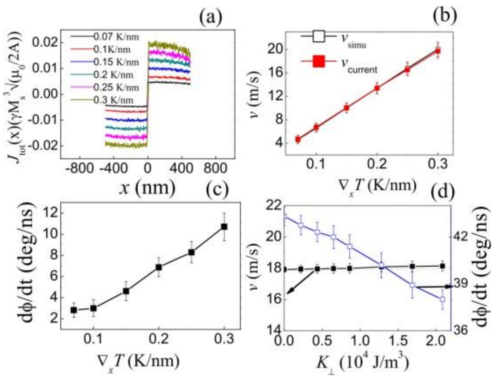

FIG C. 1. (a) Variability in spin current densities$\mathbf{J}_{tot}$(x) across different ∇_xT values. The center of the DW was selected to be x =0. (b) The reliance of DW velocity $\mathbf{v}_{simu}$ on thermal gradient in micromagnetic models (open squares) and the calculation of $v_{current}$ from the overall spin current (solid squares). (c) The reliance of DW-plane rotation angular velocity (squares) on thermal gradient. The parameters for model (a) (b) (c) included L_x = 2048 nm,L_y = L_z = 4 nm, α = 0.004 and $K_{\|}$ = 5 × 10^5J/m^3. (d)v_{simu} (solid squares) and dφ/dt (open squares) in relation to $K_{\perp}$ for L_x = 1024 nm and $\nabla_x T$ = 0.5 K/nm.

(b) Dependence of DW dynamics on damping and anisotropy: Under the given thermal gradient and the cross-section, FIG. C. 2 showed the influence of damping α on v_{simu}, $v_{current}$ and dφ/dt, FIG. C. 3 showed the dependence of v_{simu}, $v_{current}$ and dφ/dt on $K_{\|}$. The velocity at a fixed $K_{\|}$ is given.

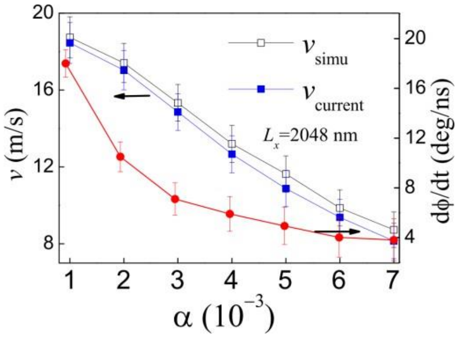

FIG. C. 2. The influence of damping α on DW dynamics was represented by: v_{simu} (Open squares); $v_{current}$ (solid squares); and dφ/dt (solid circles). The parameters of the model included $\nabla_x T$ = 0.2 K/nm, $K_{\|}$= 5 × 10^5 J/m ^{3} , L_x = 2048 nm and L_y = L_z = 4 nm.

(c) Separation of adiabatic and non- adiabatic torques: The non-adiabatic effect coefficient β, which does not change with the thermal gradient, was given as a function of α and $K_{\|}$. Then, based on the expression containing the domain wall width △~ $(A/K)^{1/2}$ (where A is the exchange coefficient) and β α, the expression of the DW plane rotation speed φ and the DW propagation speed v with respect to these coefficients is obtained.

All in all, this research took advantage of using directly simple methods and being clear on variable control. But it is also a bit weak in having not fully studied the kinematic law of the DW plane rotation speed φ under the thermal gradient.

2.4 Geometric magnonics with chiral magnetic DWs (2020) [4]

This research investigated geometric magnons in chiral domain walls.

It employed the LLG equation for magnetization direction m and derived an equation using semiclassical Lagrangian density. These yielded numerical results for fictitious electromagnetic fields of chiral DWs in normally and tangentially magnetized films, **shown in FIG. D.1.**

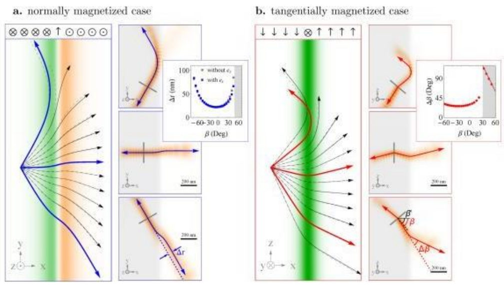

FIG. D. 1. Computational modeling of spin wave scattering caused by a chiral domain wall in (a) normally magnetized film and (b) tangentially magnetized film.

FIG. D.2. illustrated the Magnonic Snell's law, distinguishing expressions for normally vs. tangentially magnetized films by matching isofrequency circles.

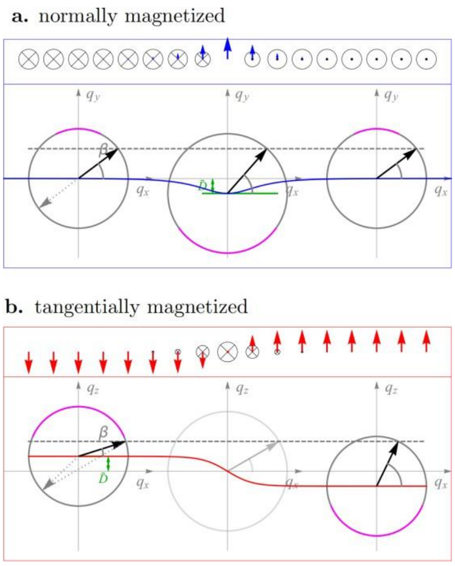

FIG. D. 2. Schematics of magnonic Snell's law across chiral domain wall in (a) normally magnetized film and (b) tangentially magnetized film.

The result of the research are as below:

(a) SPIN WAVE DEFLECTIONS BY ANTIFERROMAGNETIC DOMAIN WALL

The magnetization in two sublattices of antiferromagnets $\mathbf{m}_{1/2}$ and the staggered magnetization $\mathbf{n}$ were denoted as $\mathbf{n}=(\mathbf{m}_1-\mathbf{m}_2)/|\mathbf{m}_1-\mathbf{m}_2|$, and the net magnetization is $\mathbf{m}=\mathbf{m}_1+\mathbf{m}_2$, due to $\mathbf{n}\cdot\mathbf{m}=0$ the magnetic dynamics in antiferromagnets was defined as:

$\frac{1}{\gamma J}\mathbf{n}\times\ddot{\mathbf{n}}=-\gamma\mathbf{n}\times\mathbf{h}+\alpha\mathbf{n}\times\dot{\mathbf{n}}$ Among it $\mathbf{h}=AA^2n+Kn_z\hat{\boldsymbol{z}}-DA\times\mathbf{n}$ is the effective field, and J is the inter- sublattice exchange coupling constant.

Similar to the ferromagnetic scenario depicted in FIG. D. 1., the polarization- dependent scattering patterns **depicted in FIG. D. 3.** is easily comprehensible through the effective electromagnetic fields.

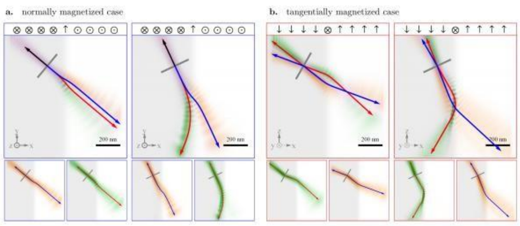

FIG. D. 4. The narrowing of spin waves due to a chiral domain wall in normally magnetized film occurred in (a) ferromagnetic and (b) antiferromagnetic settings.

In conclusion, it stressed its advantages such as providing detailed discussions on different magnetization characteristics at the geometric level, but it had a slightly stronger geometric bias in its derivation process.

2.5 Dynamics of bistable N´eel domain walls under SOT (2023) [5]

This article talked about the Dynamic of bistable N'eel domain walls and studied some of its theories by using the model of collective coordinates. It is also the main particle that is referred to by my study. Due to this reason the introduction of this article will be longer and more detailed than others.

The primary use of the collective coordinate model in this study was to depict DW actions via two factors: q-indicating the DW's location on the wire (thus its velocity $\mathbf{v}=\dot{\boldsymbol{q}}$) and φ-the angle between the DW's central magnetization and its current direction (with φ=0 or π referring to a N´eel DW and φ = π/2 or −π/2 corresponding to a Bloch DW), the initial states are decided by Q =±1 and φ_0 (can be valued as 0 or π).

The results below were carried out by this experiment:

(a) Domain wall dynamics under spin-orbit torque

N´eel wall' s movements in SOT were shown in FIG. E. 1. Among it, diagrams **depicted in FIG. E. 1. (b)** showed the trajectory of the DW motion and the evolution of φ under SOT depending on the (Q, φ_0) setup. Pertaining to a specific Q, the DW moved in up/down as Q=1 and down/up as Q=-1 contingent on φ_0.

FIG. E. 1. (c) illustrated the modeled dynamics of DW at an increased current density J when Q = 1 and φ_0 = 0. Outlines of N' eel DW in an uneven trilayer was shown in FIG. E. 1. (a)

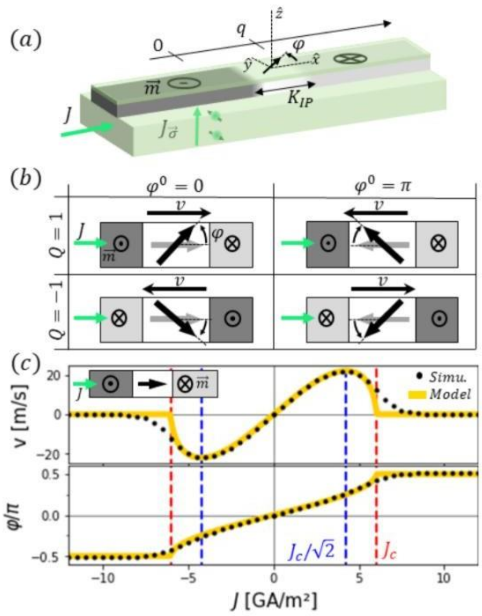

FIG. E. 1. Movement of the N´eel wall as per SOT. (a) Outline of a bistable N'eel DW within an uneven HM/FM/HM trilayer. (b) Outline how a bistable N' eel DW propagated and moved internally, influenced by the positioning of adjacent domains and the DW's starting condition. (c) Development of the DW velocity v (upper section) and its related internal angle φ (lower section) in relation to the current density J.

(b) Collective coordinate model

Integrating the LLG equation analytically, taking into account the rigid Bloch DW ansatz, resulted in interconnected motion equations:

$$\dot{q} = \frac{\triangle}{\alpha\tau_0}\left(\alpha^2 Qjcos\varphi + \frac{sin2\varphi}{2}\right)$$

$$\dot{\varphi} = \frac{1}{\tau_0}\left(Qjcos\varphi - \frac{sin2\varphi}{2}\right)$$

where △ are as DW width.

In the case of steady state motion in an asymptotic state, both the DW velocity and the internal angles remained unchanged, denoted as **v**$^\infty$ and φ^∞. These two were valued in different current density:

$$\mathbf{v}^\infty = \begin{cases} (S_1)\frac{\triangle}{\tau_0}\frac{1+\alpha^2}{\alpha} j\sqrt{1-j^2}, & if\ J < J_C \\ 0 & , if\ J \geq J_C \end{cases}$$

$$\varphi^{\infty}=\begin{cases}(\tilde{\varphi}_0)+(S_1)arcsinj, & if\ J\leq J_C\\ (S_2)\frac{\pi}{2} & ,if\ J\geq J_C\end{cases}$$

(c) Regime of transience

In the transient phase, the DW velocity's inconsistency with φ exerts significant influence. This phenomenon is most apparent near the critical current, where the modeled DW speed doesn't appear to disappear right away at J ≥ Jc, contrary to predictions in steady-state motion.

(d) Brownian motion under large current pulses

The implicit dependence of φ^{∞} on φ_0, led to DW reversal under large pulses, shown in FIG. E. 2.

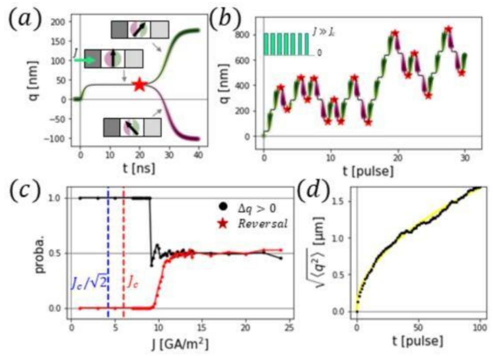

FIG. E. 2. DW's Brownian movement under intense current pulses: (a) DW reversal after pulse J_C in magnitude. (Green: $\varphi\in[-\frac{\pi}{2},\frac{\pi}{2}]$, Purple: $\varphi\in[\frac{\pi}{2},\frac{3\pi}{2}]$). (b) DW response to pulse series (20ns delay insect). (c)Calculated DW motion probability for 1000 pulses corresponding to varying current densities. (d) illustrated the progression of square root in the displacement of the mean square $\langle q^2\rangle$ averaged across 200 sequences of 100 pulses.

(e) Propagation reversal under perpendicular field

In the presence of H_z, the expression of $\dot{q}$ and $\dot{\varphi}$ in E.(b) became:

$$\dot{q}=\frac{\triangle}{\alpha\tau_0}(\alpha^2Q[jcos\varphi+h_z]+\frac{sin2\varphi}{2})$$

$$\dot{\varphi}=\frac{1}{\tau_0}(Q[jcos\varphi\ +h_z]-\frac{sin2\varphi}{2})$$

As dimensionless out-of-plate field $h_z=\frac{H_z}{\alpha H_{KIP}}$ relating to the proportion between H_z, leading to φ rotation along the QH_z axis (unrestricted by the value of φ) and H_{KIP} which typically maintains the DW in its N'eel state.

Examples of field- driven propagation reversal pulses were shown in FIG. E. 3. for pulse width of t_{H_z}= 3 ns and Q = 1 at different magnitudes (H_z > 0).

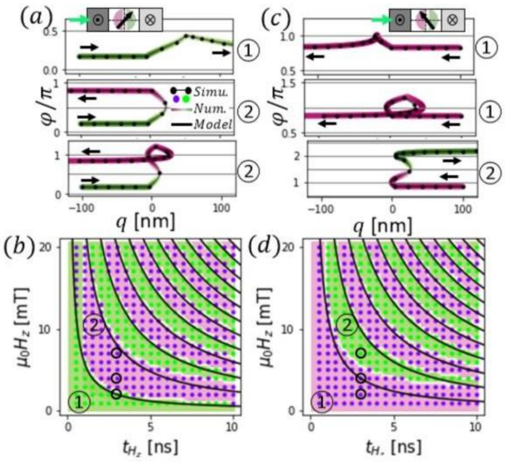

FIG. E. 3. Reversal of propagation under Hz in the (q,φ) space at pulse width of $t_{H_z} = 3$ ns and Q = 1 [(a): $\varphi^0 \in [-\frac{\pi}{2},\frac{\pi}{2}]$, (b): $\varphi^0 \in [\frac{\pi}{2},\frac{3\pi}{2}]$].

(f) Step in anisotropy

The experiment achieved effects which out-of-plane field had the propagation reversal allowance, and the DW propagation was disturbed significantly with multiple reversals through took a spatial variation of the out-of-plane anisotropy K(x) (where x represents the wire's position), potentially linked to a significant local out-of-plane field being contemplated.

$$H^K_{z(q)} = -\frac{\Delta}{\mu_0 M_S} \partial_q \tilde{K}_{(q)}$$

$$K_{(q)} = \frac{\int K(x)(1-m^2_{x,(x,g)})dx}{\int (1-m^2_{x,(x,g)})dx}.$$

The impact of a δK magnitude anisotropy step at the position x_{step} on a moving DW was illustrated in FIG. E. 4. under the scenario where $Q = 1$ and $\varphi^0 = \varphi^\infty$ varying J and different step magnitudes.

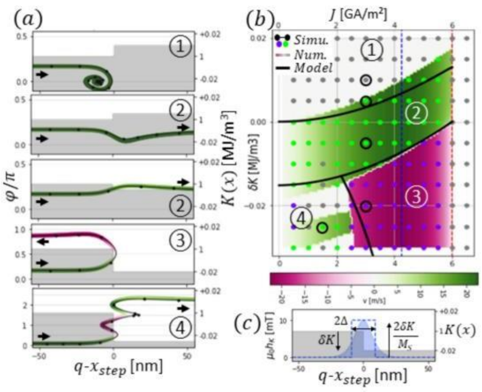

FIG. E. 4. Reversal of propagation during an anisotropy phase: (a) illustrated the reversal of a DW's propagation at the anisotropy phase, specifically at the x_{step} position in the (q, φ) space for $\varphi^0 = \varphi^\infty$, Q = 1 and varying (J, δK). (b) illustrated the reversal phase diagram within the (J, δK) space. (c) estimated the effective field $H^K_{z(q)}$ in a distinct manner.

(g) Finite magnetic track

(b) and (c) in FIG. E. 5. demonstrated that a comparable outcome is achievable at the ends of a limited magnetic wire,indicated by black dots in (c) of FIG. E. 5. exhibited a response to the DW's simulated path in (q, φ) space, with the background hue matching the magnetic element's form.

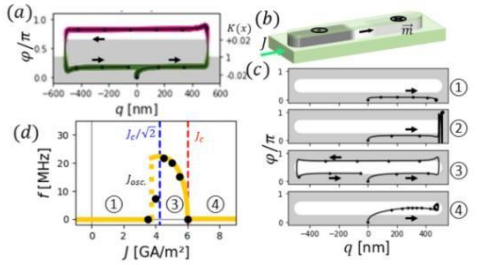

FIG. E. 5. (a) DW oscillation between anisotropy steps under steady current. (b) DW oscillator schematic (Q = 1, φ^0 = 0). (c) DW's actions (as halted, annihilated, or mirrored) by the extremities of the track in the (q,φ) space. (d) The fluctuation in the frequency of DW oscillations corresponding to varying levels of the DC current derived from DW actions.

It provided very detailed theories of bistable N'eel DW Dynamic under SOT with its images of research results, but it made some mistakes that cannot be ignored. It is not available to calculate DW Dynamic accurately by using just two parameters without using their meaning to conclude different situations.

2.6 Dynamics of magnetization at infinite temperature in a Heisenberg spin chain (2024) [6]

This research studied by using Heisenberg XXZ spin chain which describes the nearest-neighbor exchange interactions between spin-1/2 particles with the **Hamiltonian** as their **basic model**:

$$\mathrm{H} = \sum_i (S_i^X S_{i+1}^X + S_i^Y S_{i+1}^Y + \triangle\, S_i^Z S_{i+1}^Z)$$

Where S^X, S^Y and S^Z are spin $-\frac{1}{2}$ operators and $\triangle$ is the anisotropy parameter. Only if $\triangle$=1 can this system be the Heisenberg model.

By using this model to simulate in a 1D chain it calculated around cycle unitary as U_F and used this to derive the transferred magnetization M. FIG. F. 1. showed the DW relaxation by using this model.

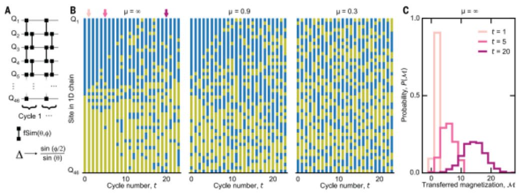

FIG. F. 1. Relaxation of DW within the Heisenberg XXZ spin chain. (A)Unitary gate sequence (B) The behavior of relaxation in relation to the site and the number of cycles. (C)Likelihood distribution of magnetization transfer histogram after t = 1, 5, and 20 cycles for μ= ∞.

This research also used **statistic physics** as tool to **analyze** transferred magnetization's **mean and variance**.

The result of mean and variance of transferred magnetization in different situations was shown as FIG. F. 2.

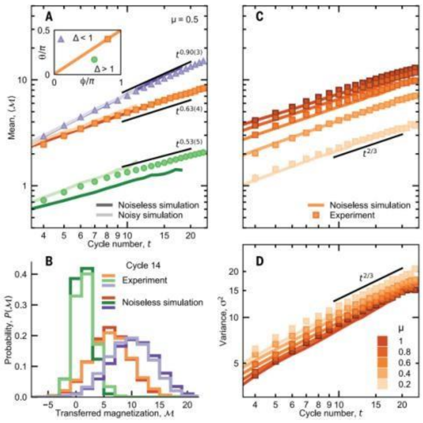

FIG. F. 2. Mean and variance across different transportation systems. (A)Mean of transferred magnetization ⟨M⟩ which was a function of cycle number (t) for initial states with μ = 0.5 and for △, (B) Histogram depicting P(M) for D values examined in (A) during cycle 14. (C) Mean and (D) variance of M for △= 1 and 0.2 ≤μ≤ 1, ranging from righter to darker squares.

Besides this research, I also did some further studies to analyze skewness S and kurtosis Q of P(M) as higher order moments. The total experiment result can be seen in FIG.F.3.

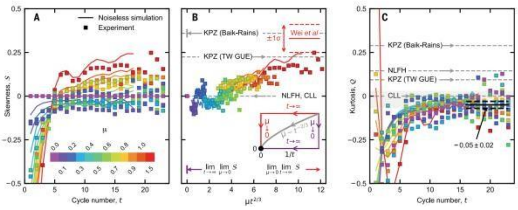

FIG. F. 3. Skewness and excess kurtosis in the magnetization transfer. (A) Skewness of transferred magnetization distribution S as a function of t, for △ = 1 and different μ values. (B) Identical to (A), yet with the x-axis adjusted to $\mu t^{2/3}$ and omitting data points where t < 8. (C) Kurtosis Q in the magnetization transfer.

Though it has the drawback of being insufficient in-depth exploration of dynamic properties, but it did a great job on introducing a large amount of statistical physics compared to general domain wall-related dynamics research, with strong methodological innovation. Also, it was excellent for color distinguishing and figuring results of experiments more directly when coming into its figures.

2.7 Conclusion

All in all, those researches all worked on the characteristics of DW in different conditions, and they did have great effects on polishing and widening the theory of DW Dynamic, among them most of them referred the basic theories of magnetic physics such as LLG equation, besides, different researches also referred different physics sub-types such as quantum physics, statistics physics and thermal physics, but those didn' t study DW in a more microscopic and more universal way. Due to this fact I advise to widen and polish DW Dynamic by using more theories of statistic physics and paying more attention on the micro characteristics of DW by researching spin waves in it more frequently or taking more attention on the interaction between Domains or between a Domain and other objects to study their influences on DW. Besides using statistics physics or quantum mechanics to expand DW Dynamic is very helpful to research it.

3. Assumption and comparison

3.1 Assumption

After Introducing the brief history of studying the laws of Domain Wall Dynamic in different ways, in this item I would like to assume some part of Bloch DW Dynamic when not influenced by DMI and external magnetic field.

First of all, due to the mistakes of only using position-q and angle-φ when using collective coordinates [7] to study the dynamic of N'eel DW in SOT environment, I'd like to correct the mistakes the previous author made by the way, by using the mean values of q and φ instead of themselves, we can express the dynamic characteristic of Bloch DW driven by SOT as well.

There I would like to give the assumed expression of $\langle q\rangle$ and $\langle\varphi\rangle$ by using statistic physics:

$$\langle \mathrm{q}\rangle = \int \mathrm{qP}(\mathrm{q},\varphi,\mathrm{t})\mathrm{dqd}\varphi$$

$$\langle \varphi\rangle = \int \mathrm{qP}(\mathrm{q},\varphi,\mathrm{t})\mathrm{dqd}\varphi$$

Among these two expressions, P(q,φ,t) is a form of probability density function.

This step we have defined the basic form of $\langle q\rangle$ and $\langle\varphi\rangle$,but it is necessary to make a correlation to express more accurate forms of $\langle q\rangle$ and $\langle\varphi\rangle$ by using LLG equation:

$$\frac{d\boldsymbol{m}}{dt} = -\gamma_0 \boldsymbol{m}\times\boldsymbol{H}_{eff} + \alpha\boldsymbol{m}\times\frac{d\boldsymbol{m}}{dt} + \tau_{SOT} + \eta \text{ [9]}$$

Among this equation the τ_{SOT} is the characteristic time scale of SOT and the η[9] is Gaussian white noise term, the value of η is decided by the Fluctuation -Dissipation law.

As for the Langevin form we added the random magnetic field intensity as $\boldsymbol{H}_{th}$, it fits conditions below:

$$\langle H_{th,i}(t)\rangle = 0$$

$$\langle H_{th,i}(t)H_{th,j}(t')\rangle = \frac{2k_BT\alpha}{\gamma_0\mu_0M_sV}$$

Due to the fitness of those conditions, we can renew the expressions of $\langle q\rangle$ and $\langle\varphi\rangle$ by using their derivative forms as:

$$\frac{d\langle q\rangle}{dt} = \frac{\triangle}{\alpha\tau_0}\left(\alpha^2Qjcos\langle\varphi\rangle + \frac{sin2\langle\varphi\rangle}{2}\right) + \zeta_q(t)$$

$$\frac{d\langle\varphi\rangle}{dt} = \frac{1}{\tau_0}\left(Qjcos\langle\varphi\rangle - \frac{sin2\langle\varphi\rangle}{2}\right) + \zeta_\varphi(t)$$

Since we are studying Bloch DW which characteristics are shown in Part 1., When SOT has the driving current $J>J_C$, the value of $\langle\varphi\rangle$ can be fixed as $\pm\frac{\pi}{2}$ as the Bloch DW' s intrinsic property (if $J\leq J_C$ the sub-type of DW cannot be fixed as Bloch DW, but in this part we only discuss about the dynamic of Bloch DW in SOT environment), in this condition we have $\frac{d\langle q\rangle}{dt} = \zeta_q(t)$ and $\frac{d\langle\varphi\rangle}{dt} = \zeta_\varphi(t)$, among these, $\zeta_q(t)$ and $\zeta_\varphi(t)$ are Gaussian white noise term, they fit:

$$\langle\zeta_i(t)\rangle=0,\langle\zeta_i(t)\zeta_i(t')\rangle=\delta(t-t'),$$

$$i=q,\varphi.$$

This shows that the SOT cannot drive Bloch DW to move but the heat noise can cause the value of q and φ moving. From the Fokker-Planck equation [8] to define the probability density function we have:

$$\frac{\partial P}{\partial t} = -\frac{\partial}{\partial q}[A_qP] - \frac{\partial}{\partial\varphi}[A_\varphi P] + D_q\frac{\partial^2P}{\partial q^2} + D_\varphi ,$$

and by using the Fluctuation-Dissipation law we can calculated that the diffusion coefficients are $D_q = \frac{k_BT}{\Gamma_g}$, $D_\varphi = \frac{k_BT}{\Gamma_\varphi}$ [10], among these Γ_q and Γ_φ are the effective damping coefficient.

Using LLG equation to estimate the diffusion coefficients we have:

$$D_q \approx \frac{k_BT\triangle}{\alpha\gamma_0\mu_0M_SV} \text{ [11]}$$

$$D_\varphi \approx \frac{k_BT}{\alpha\gamma_0\mu_0M_SV}$$

In conclusion, when ignoring the disturb brought by Gaussian white noise, since that the value of drift term is zero, we can consider that $\frac{d\langle q\rangle}{dt}$=0 and $\frac{d\langle \varphi\rangle}{dt}$=0, this means that the mean value of position and angle remain unchanged, while the equation of diffusion has the form showed below:

$$\langle [q(t) - \langle q \rangle]^2 \rangle = 2D_q t$$

$$\langle [q(t) - \langle q \rangle]^2 \rangle = 2D_\varphi t$$ [12]

The value of D_q and D_φ are the same as the estimated value calculated by LLG equation. This means that the value of q and φ have a linear relationship with t.

3.2 Comparison

Compared with N' eel DW which pure status has $\langle \varphi \rangle$=0 in right rotation and π in left rotation. Unless the DW is fixed on Bloch sub-type by letting driving current $J>J_C$, the value of drift term would not be zero. This means that SOT can only drive N' eel DW effectively, instead pure Bloch DW can only move in the condition of existing white noises.

4. Conclusion and Perspectives

From Part 2. (This part I gave detailed conclusion in Sub-part G.) and Part 3. I concluded six research projects on DW Dynamic in last 15 years, and especially I made some assumptions by referring to research E. and made some assumptions Bloch DW Dynamic in SOT. Though these assumptions should be proved by experiment one day, and until nowadays the DW Dynamic needs plenty of process to move ahead, there does exist plenty place to correct my theory, I hope these may inspire readers and to wonder processes of DW Dynamic research inspire me.

REFERENCES

[1] All-Magnonic Spin-Transfer Torque and Domain Wall Propagation, By R.Pan, X.S.Wang and X.R.Wang, 2011.
[2] Universal magnetic domain wall dynamics in the presence of weak disorder, By Jacques Ferré, Peter J. Metaxas, Alexandra Mougin, Jean-Pierre Jamet, Jon Gorchon, Vincent Jeudy, 2013.
[3] Thermal gradient driven domain wall dynamics, M. T. Islam, X. S. Wang, X. R. Wang, 2018.
[4] Geometric magnonics with chiral magnetic domain walls, By Jin Lan, WeichaoYu and Jiang Xiao, 2020.
[5] Dynamics of bistable N´eel domain walls under spin-orbit torque,By Eloi Haltz,K´evin J. A. Franke and Christopher H. Marrows， 2023.
[6] Dynamics of magnetization at infinite temperature in a Heisenberg spin chain,By E. Rosenberg,T. I. Andersen,A. Petukhov,D. Abanin,etc.,at KPZ University,published on Science on 5 April 2024.
[7] The Motion of 180°Domain Walls in Uniform DC Magnetic Fields, By N. L. Schryer, L. R. Walker, 1974.
[8] Thermal Fluctuations of a Single-Domain Particle, By W. F. Brown, 1963.
[9] Domain Wall Motion by the Magnetoelastic Effect, By D. Hinzke, U. Nowak, 2011.
[10] Thermally Activated Domain Wall Dynamics in Perpendicular Anisotropy Films, By J. M. L. Beaujour, D. Ravelosona, J. A. Katine, 2006.
[11] Thermal Effects on Domain Wall Mobility under Spin-Orbit Torque, By S. Emori, U. Bauer and G. S. Beach, 2014.
[12] Thermally Activated Domain Wall Dynamics under Spin-Orbit Torque, By dominant author K. J. Kim and other authors, 2018.